

## Supporting Information

### **Progressive stress response of the anaerobic granular sludge to nickel nanoparticles: Experimental investigations and mathematic modelling**

Chuan-Shu He<sup>a#</sup>, Liang Huang<sup>a#</sup>, Rong-Rong Ding<sup>a</sup>, Hou-Yun Yang<sup>a,b</sup>, Yi-Xuan Wang<sup>a</sup>, Jie Li<sup>a</sup>, Yang Mu<sup>a,\*</sup>

<sup>a</sup>CAS Key Laboratory of Urban Pollutant Conversion, Collaborative Innovation Centre of Suzhou Nano Science and Technology, Department of Applied Chemistry, University of Science and Technology of China, Hefei, China

<sup>b</sup>School of Environment and Energy Engineering, Key Laboratory of Anhui Province of Water Pollution Control and Wastewater Reuse, Anhui Jianzhu University, Hefei, China

#### **\*Corresponding author:**

Prof. Yang Mu, E-mail address: [yangmu@ustc.edu.cn](mailto:yangmu@ustc.edu.cn)

<sup>#</sup>These authors contributed equally to this work.

## **1. Materials and methods**

### **1.1 Ni-NP synthesis and characterization**

Briefly, the reductant was prepared by dissolving 14.16 g of NaBH<sub>4</sub> and 1 g of NaOH in 500 mL of purified water, which was sparged with N<sub>2</sub> for 20 mins in advance. In addition, 38.64 g of NiCl<sub>2</sub>·6H<sub>2</sub>O was added to a 500 mL mixture of ethanol and water ( $V_{\text{ethanol}}/V_{\text{water}} = 4:1$ ); then transferred to a three-necked bottle. A NaBH<sub>4</sub> reducing agent solution was slowly dripped into a nickel chloride solution under highly purified N<sub>2</sub> with mechanical stirring at 600 rpm at room temperature. After the reductant titration was finished, the products were washed five times with ethanol and dried overnight at 65 °C under vacuum.

The morphology of the synthesized nano-Ni particles was imaged with transmission electron microscopy (TEM) (JEM-2010, JEOL Ltd., Japan). X-ray diffraction (XRD) tests were performed using a Rigaku TTR-III with Cu K $\alpha$  radiation (Rigaku Corp., Japan). The results are shown in Fig. S1.

### **1.2 Scanning electron microscopy**

The surface morphology of the AGS exposed to (0, 200, and 600) mg/g-TSS of Ni-NPs was characterized from images made with scanning electron microscopy (SEM) (Sirion 200, FEI Ltd., USA). According to the process developed in a previous study,<sup>1</sup> 5-10 granules were taken from each reactor after AGS exposure to Ni-NPs for a month; then washed three times with 0.1 M phosphate buffer (pH 7.4). After this, they were fixed in 0.1 M phosphate buffer containing 3.0% glutaraldehyde (pH 7.4) overnight at 4 °C. Next, the granules were again washed three times with 0.1 M phosphate buffer before being fixed for 2 h in 1% osmic acid. After being washed three more times in 0.1 M phosphate buffer, each granule was dehydrated in an

ethanol series 30, 50, 70, 90, and 100% for 30 min per step. As preparation for the SEM, each granule was fixed to a copper plate using plastic electrical tape.

### **1.3 High-throughput 16S rRNA gene sequencing analysis**

Sludge samples were collected after two month operation using glucose as carbon source in the absence and presence of 600 mg/g-TSS Ni-NPs, respectively. Total genomic DNA was extracted employing the Power Soil™ DNA isolation kit (Molecular Bio Laboratories Inc., USA) according to the manufacturer's instructions. The total genomic DNA was amplified using the 16S rRNA bacteria primers that covers the V3 and V4 regions of the 16S rRNA gene: modified 341F (CCTAYGGGRBGCASCAG)/806R (GGACTACNNGGGTATCTAAT).<sup>2</sup> Primers of bacterial and archaeal region for different samples in this study were individually barcoded to enable multiplex sequencing. The PCR amplification was administered in 0.2-mL PCR tubes with T100™ Thermal Cycler (BioRad, USA). Then the PCR products were paired-end sequenced on the platform of Illumina Hiseq 2000 (Illumina, USA).<sup>3</sup> Finally, to analyze microbial community structure, the resulting high quality sequences were processed to generate operational taxonomic units (OTUs) and allocated down to the kingdom, phylum, class, order, family, and genus level through Mothur program.<sup>4</sup>

### **1.4 Other analysis**

All the samples were obtained for analysis at appropriate time intervals. 2 mL liquid sample was collected and filtered using a 0.45 mm microfilter for aquatic chemical analysis. After being acidified with 3% (v/v) HCOOH, volatile fatty acids (VFAs) including acetic acid, propionic acid, butyric acid and hexanoic acid were measured

by a gas chromatograph (Agilent 7890, USA).<sup>5</sup> The glucose concentration was determined with a high-performance liquid chromatography (HPLC) (Agilent 1260 Infinity, USA) with a refractive index detector (RID) and a Hi-Plex H column (300 × 7.7 mm). Column temperature was 55 °C using 5 mM H<sub>2</sub>SO<sub>4</sub> as eluent at a flow rate of 0.6 mL/min.<sup>6</sup> VSS and COD were analyzed according to the standard methods.<sup>7</sup> The concentrations of Ni<sup>2+</sup> in the solution during experiments process were analyzed via atomic absorption spectrum (Analyst 800, Perkin Elmer, USA). The EPS in the sludge was extracted by employing the cation exchange resin method.<sup>8</sup> Afterwards, the concentrations of polysaccharides and protein comprised in EPS were assayed by applying a sulfuric acid-anthrone method and bicinchoninic acid (BCA) protein assay kit (Sangon Co., China), respectively.<sup>9</sup> The extracted EPS solution was further freeze-dried for 48 h prior to FTIR spectroscopy analysis to characterize the major functional groups of EPS and their interaction with Ni-NPs.<sup>1</sup> 1 mg freeze-dried EPS samples and 100 mg dried KBr were then homogenised in an agate grinder, further compressed and analysed by a FT-IR spectrometer (Nicolet 6700, Thermo Electron Corporation, USA) within a spectral range of 4000–400 cm<sup>-1</sup>, 16 scans and a resolution of 4 cm<sup>-1</sup>.<sup>10</sup>

## **2. Results**

### **2.1 Characterization of prepared Ni-NPs**

As shown in Fig. S1a, the freshly synthesized Ni-NPs were shown to be a nano-chain with an average size of approximately 15 nm. The original XRD peaks of the synthesized nanoparticles were clearly multi-fitted. According to the integrated XRD data (Fig. S1b), the diffraction peaks at  $2\theta = 44.8^\circ$  and  $51.8^\circ$  could be assigned to the characteristic (111) and (200) planes of face-centered cubic (fcc) Ni phase (JCPDS

04–0850).<sup>11</sup> Other small diffraction patterns were well indexed to hexagonal Ni(OH)<sub>2</sub> (JCPDS 14-0117) and crystalline NiO (JCPDS 78-0643).<sup>12, 13</sup>

## **2.2 FTIR analysis of EPS**

The peak at 1640 cm<sup>-1</sup> and 1540-1570 cm<sup>-1</sup> corresponded to amido-I and -II bands of proteins, respectively (Table S1, Supporting Information), while the band near 1450 cm<sup>-1</sup> was attributed to deformation vibration of CH<sub>2</sub> and CH<sub>3</sub> in proteins.<sup>14</sup> The band near 1400 cm<sup>-1</sup> was attributed to the symmetric stretching of C=O and 1240 cm<sup>-1</sup> was related to deformation vibration of C=O in COO<sup>-</sup>. A doublet at 1100 and 1050 cm<sup>-1</sup> were assigned to C-O-C and C-H stretching in polysaccharides and/or nucleic acids. Additionally, another three peaks located at 1320, 1240, and 1010 cm<sup>-1</sup> originated from the S-O stretching, N-H bending and C-N stretching, P=O stretching vibrations, respectively.<sup>14, 15</sup> Bands at “fingerprint zone” (800-880 cm<sup>-1</sup>) might be associated with phosphate group, a functional group of which nucleic acids are composed.<sup>16</sup>

**Table S1** Effects of Ni-NPs and Ni<sup>2+</sup> additions on EPS compositions of the AGS

Experiment	Concentration (mg/g-VSS)	
	Polysaccharide	Protein
Without Ni-NPs	27.59 ± 2.34	62.81 ± 3.82
200 mg/g-TSS Ni-NPs	32.73 ± 1.37	69.33 ± 6.21
600 mg/g-TSS Ni-NPs	44.02 ± 1.40	103.78 ± 8.69
120 mg/L Ni <sup>2+</sup>	40.16 ± 1.41	92.54 ± 7.55

**Table S2** Main functional groups observed from FT-IR spectra of EPS studied <sup>1, 14-16</sup>

Wave number (cm <sup>-1</sup> )	Vibration type	Functional type
3400	Stretching vibration of OH	OH into polymeric compounds
2920-2960	Asymmetric stretching vibration of CH <sub>2</sub>	
1640	Stretching vibration of C=O and C–N (Amide I)	Proteins (peptidic bond)
1540-1570	Stretching vibration of C–N and deformation vibration of N–H (Amide II)	Proteins (peptidic bond)
1450	Deformation vibration of CH <sub>2</sub> and CH <sub>3</sub>	Proteins
1400	Stretching vibration of C=O	Carboxylates
1320	S-O stretching vibration	
1240	Deformation vibration of C=O	Carboxylic acids
1100	Stretching vibration C–O–C	Polysaccharides and/or nucleic acids
1050	Stretching vibration of O-H	Polysaccharides and/or nucleic acids
1010	P=O	ester PO <sub>2</sub> -
800-880	Phosphate groups	nucleic acids
675	Fingerprint region	

**Table S3** Comparison of the richness and diversity of the 16S rRNA gene libraries based on 0.03 distance.

	OTUs	Shannon Diversity	Chao 1 richness estimation	Goods coverage (%)
Control	451	5.234	480	99.9
600 mg/g-TSS Ni-NPs	427	4.152	463	99.8

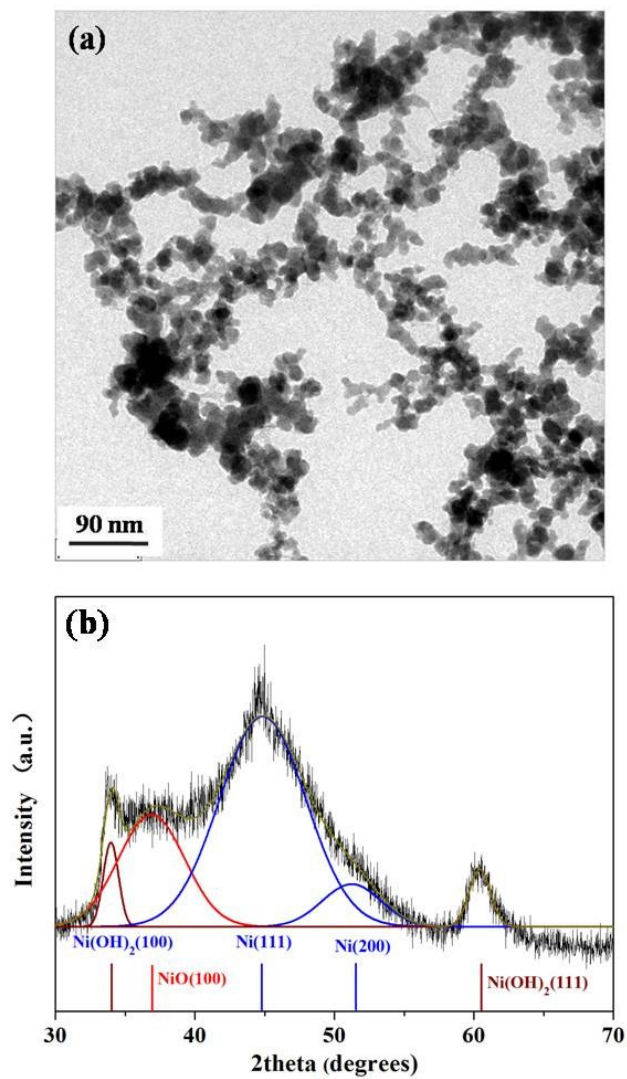


**Fig. S1** Characterization of freshly prepared Ni nanoparticles: (a) TEM, (b) XRD.

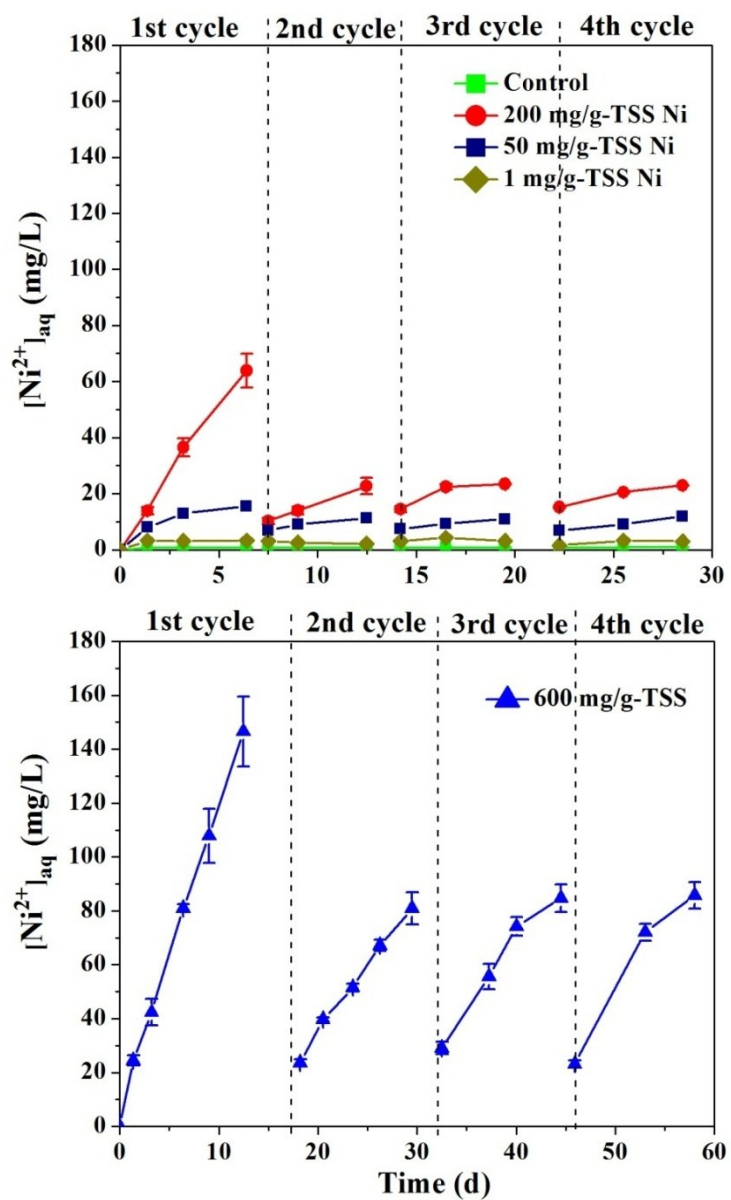


**Fig. S2**  $\text{Ni}^{2+}$  ions released from the Ni-NPs during four cycles. The time was recorded from the addition of Ni-NPs. 2 g/L glucose initial pH 7.3, 115 rpm, 35 °C.

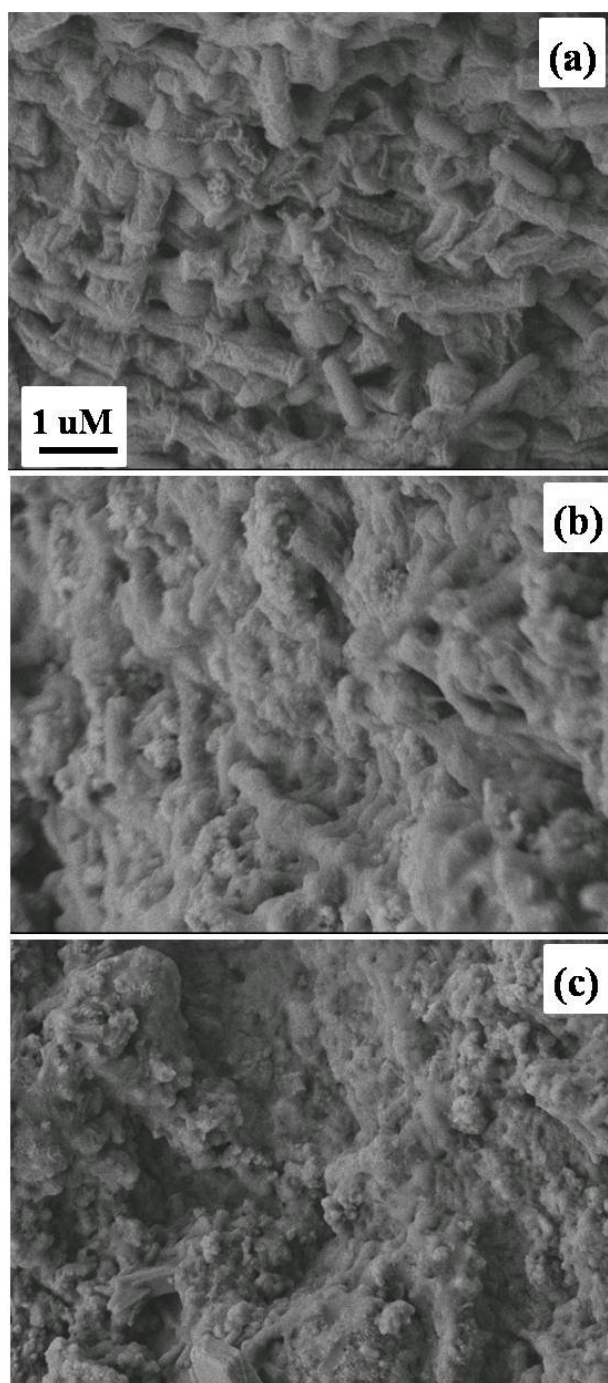


**Fig. S3** SEM graphs of AGS surface in the control (a), and in the reactor exposure to 200 mg/g-TSS Ni-NPs (b) and 600 mg/g-TSS Ni-NPs (c) after reaction for about 500 h. 2 g/L glucose, initial pH 7.3, 115 rpm, 35 °C.

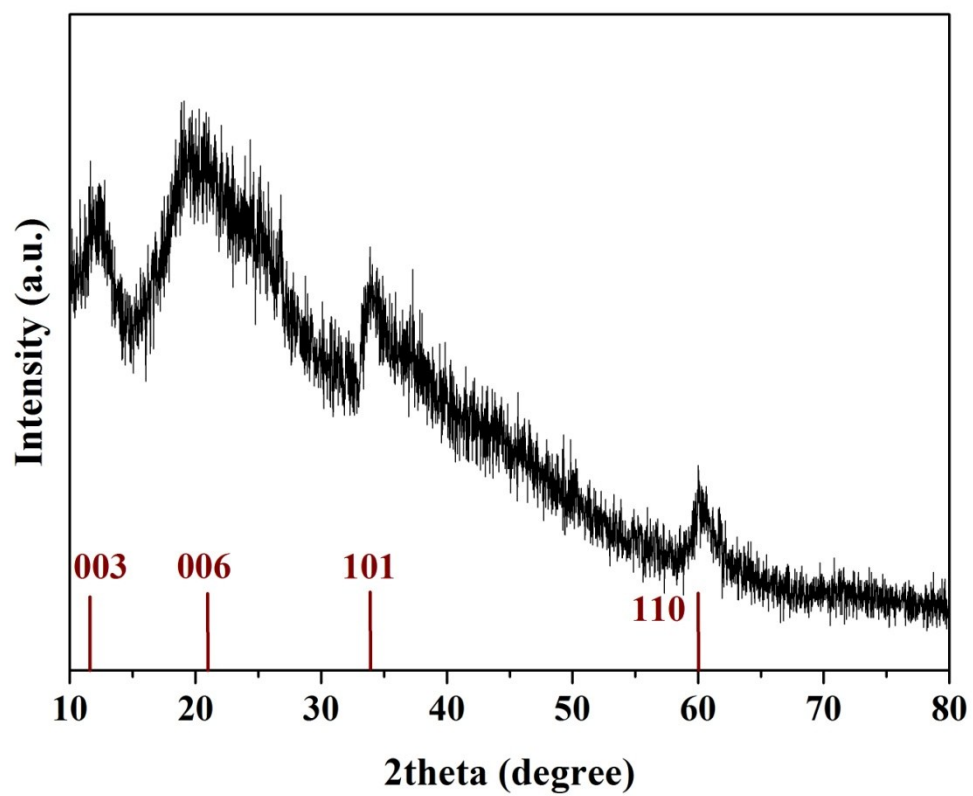


**Fig. S4** XRD result of the freeze dried anaerobic granular digestion after long-term exposure to 600 mg/g-TSS Ni-NPs.

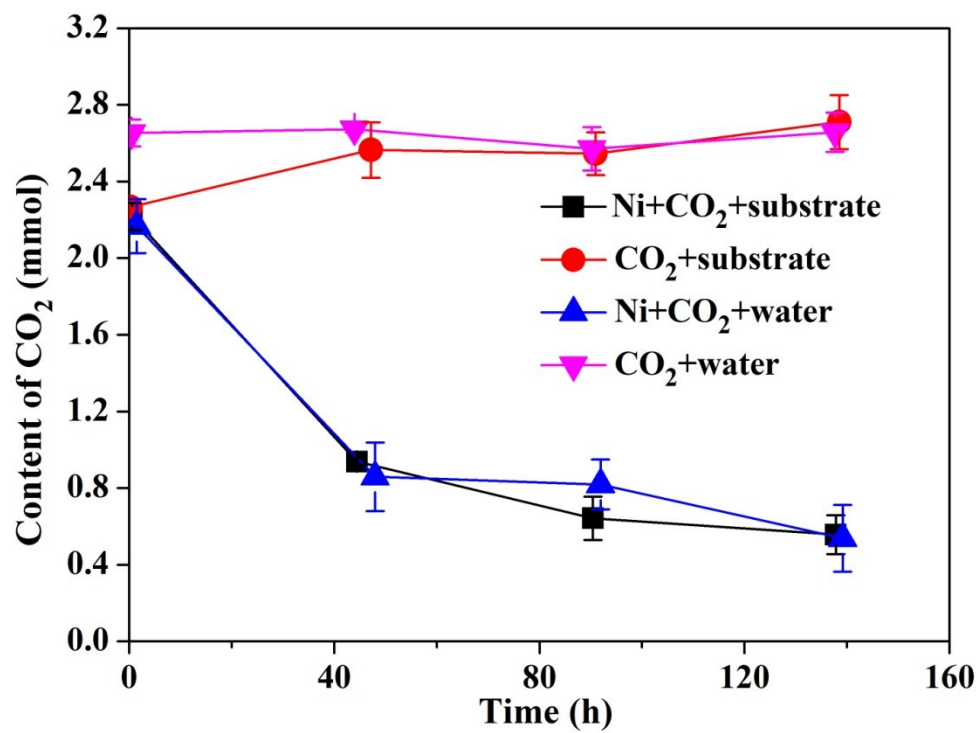
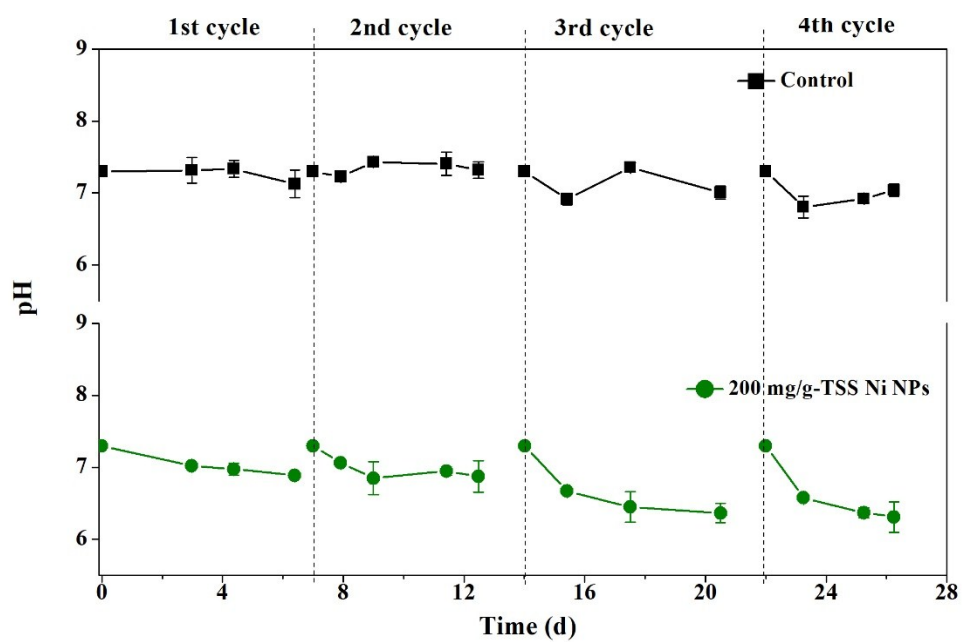
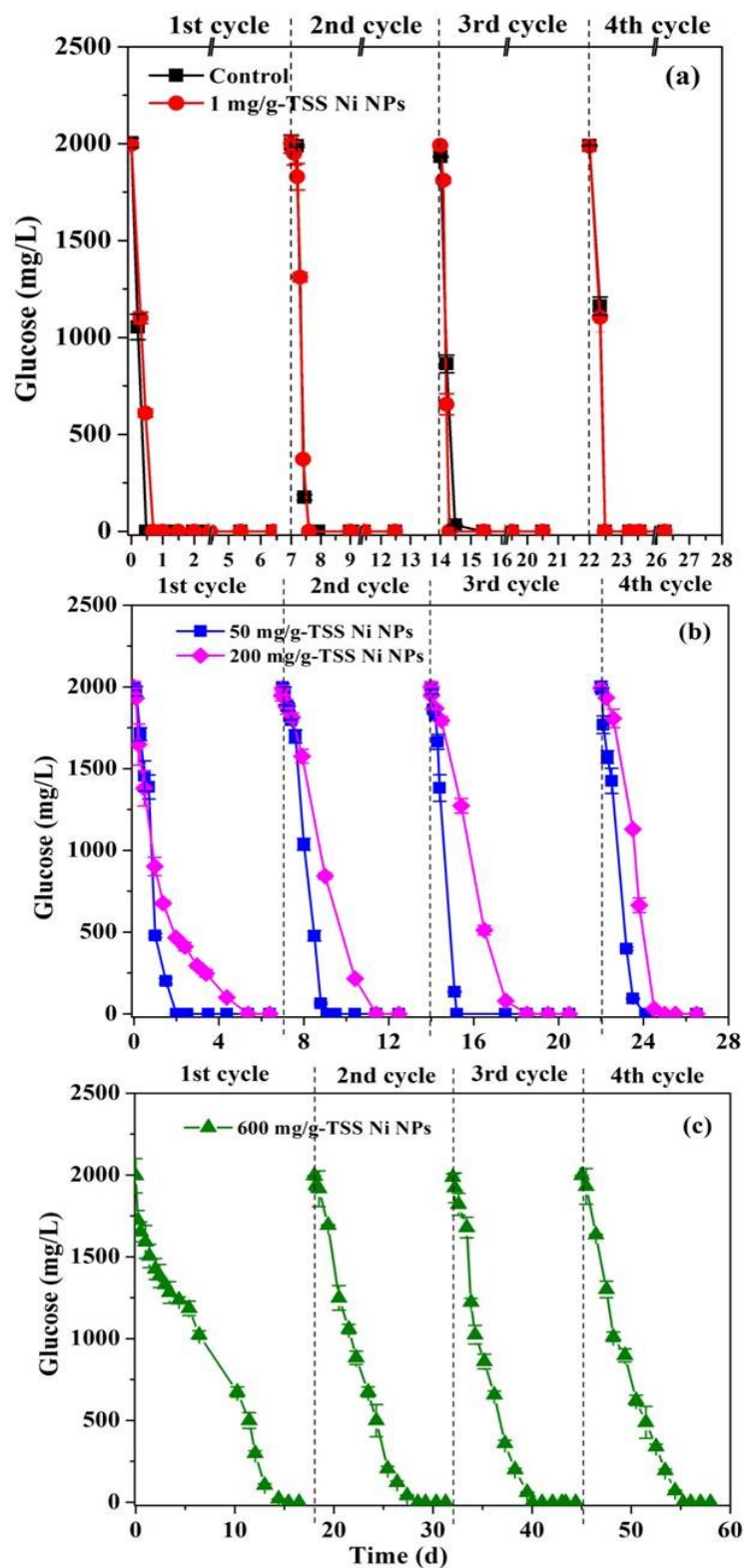


Fig. S5 CO<sub>2</sub> consumption in different kind of solutions.



**Fig. S6** pH variations of the AGS systems over long-term exposure to 0 and 200 mg/g-TSS Ni-NPs.



**Fig. S7** Effect of Ni-NPs on the glucose degradation of the AGS. Error bars represent standard deviations of triplicate tests. 2 g/L glucose, pH 7.3, 115 rpm, 35 °C.

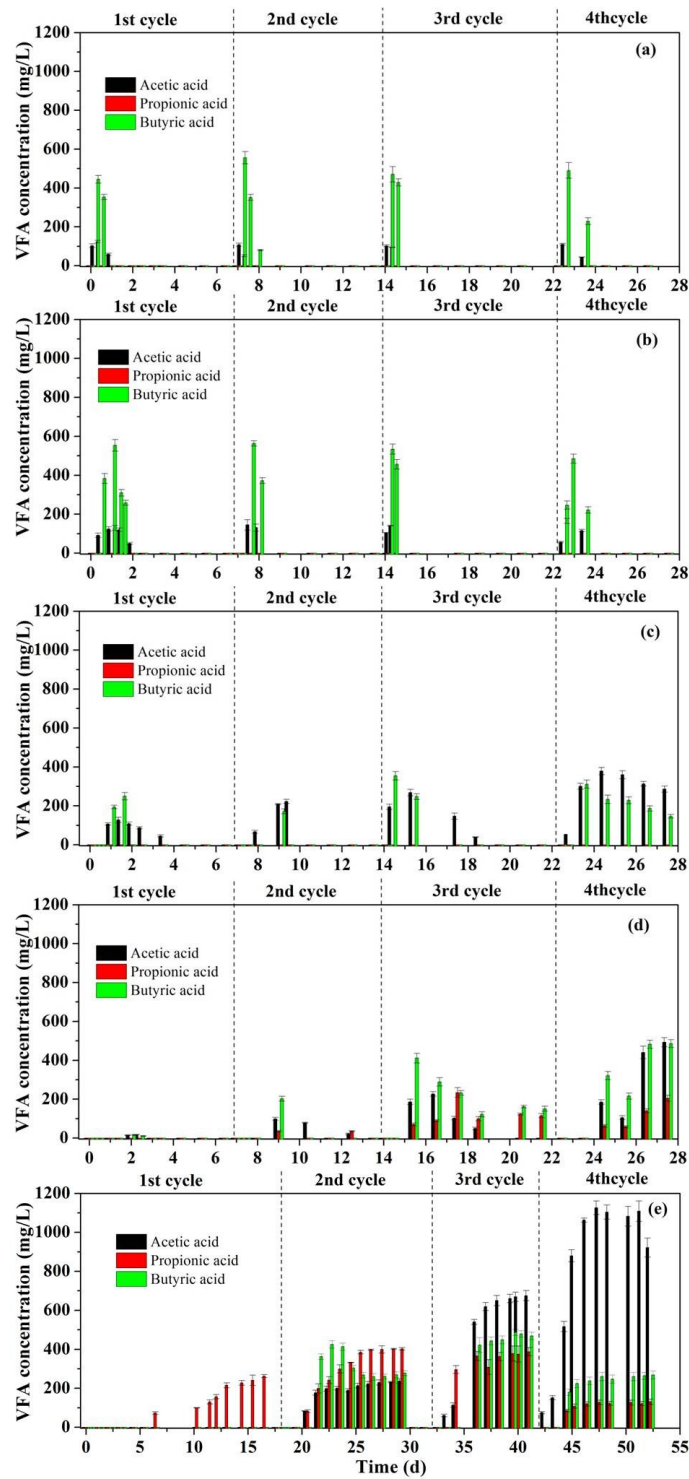


**Fig. S8** The main acidification products (including acetic, propionic and butyric acids) with time during four cycles after exposure to 0 (a), 1 (b), 50 (c), 200 (d) and 600 (e) mg/g-TSS Ni-NPs. Error bars represent standard deviations of triplicate tests. 2 g/L glucose, pH 7.3, 115 rpm, 35 °C.

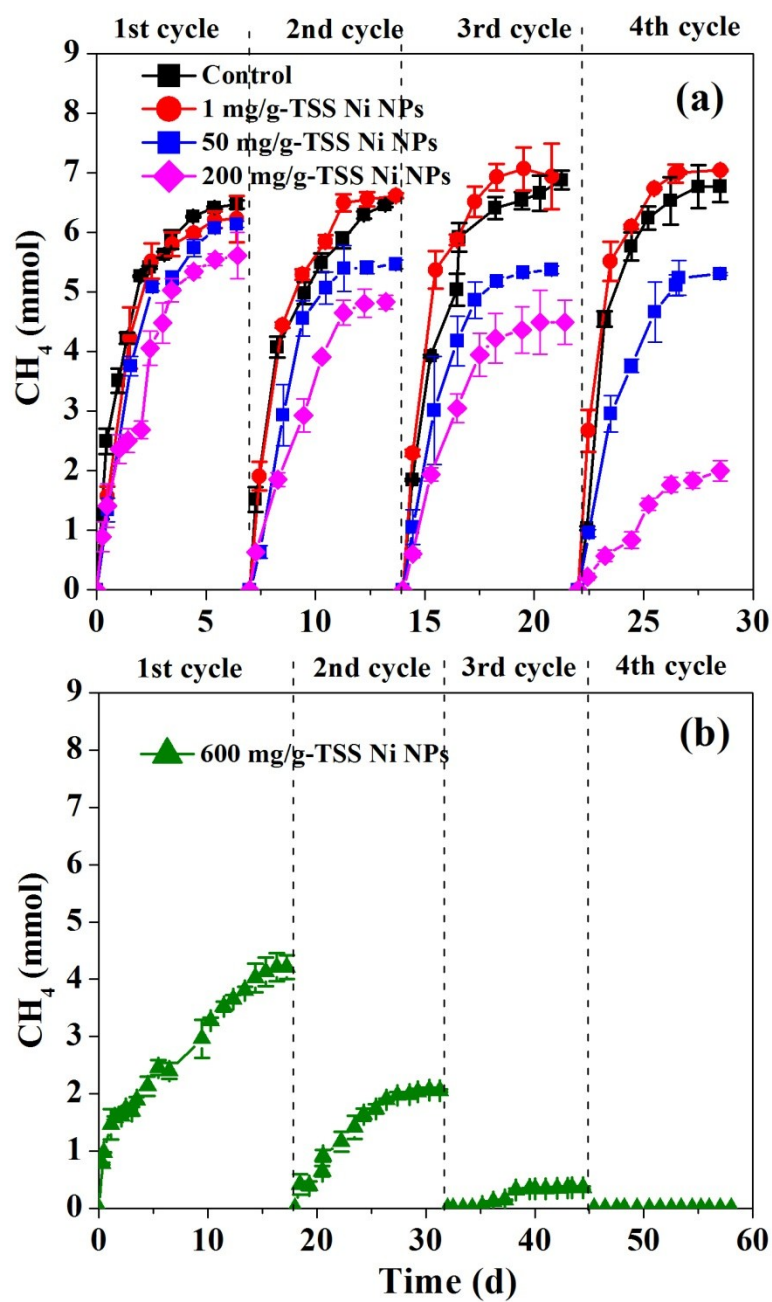


**Fig. S9**  $\text{CH}_4$  production with exposure time and concentrations of Ni-NPs during the glucose degradation systems. 0 and 1, 50 and 200 mg/g-TSS Ni-NPs (a); 600 mg/g-TSS Ni-NPs (b). The time was recorded from the addition of Ni-NPs. 2 g/L glucose, pH 7.3, 115 rpm, 35 °C.

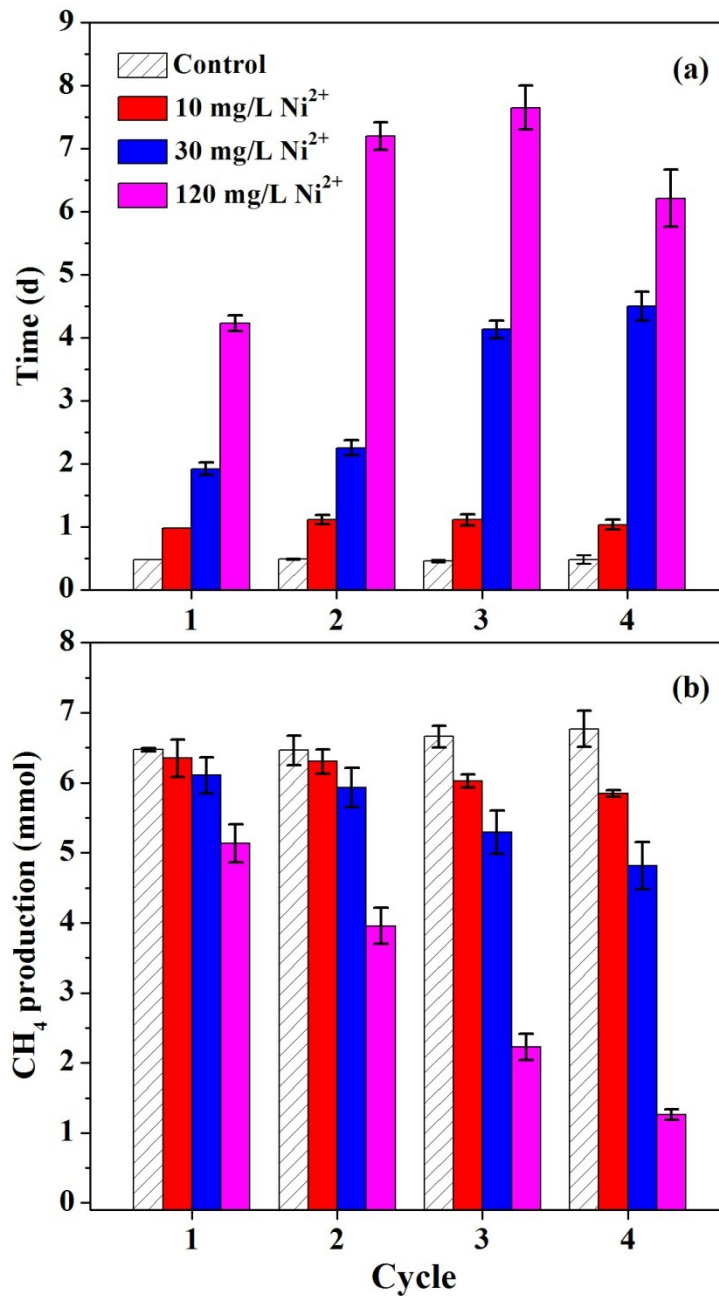


**Fig. S10** Effect of Ni<sup>2+</sup> on the activity of anaerobic granular sludge. time required for 2 g/L glucose complete removal (a) and the methane production at time of 6 day for four cycles (b). Error bars represent standard deviations of triplicate tests. 2 g/L glucose, pH 7.3, 115 rpm, 35 °C.

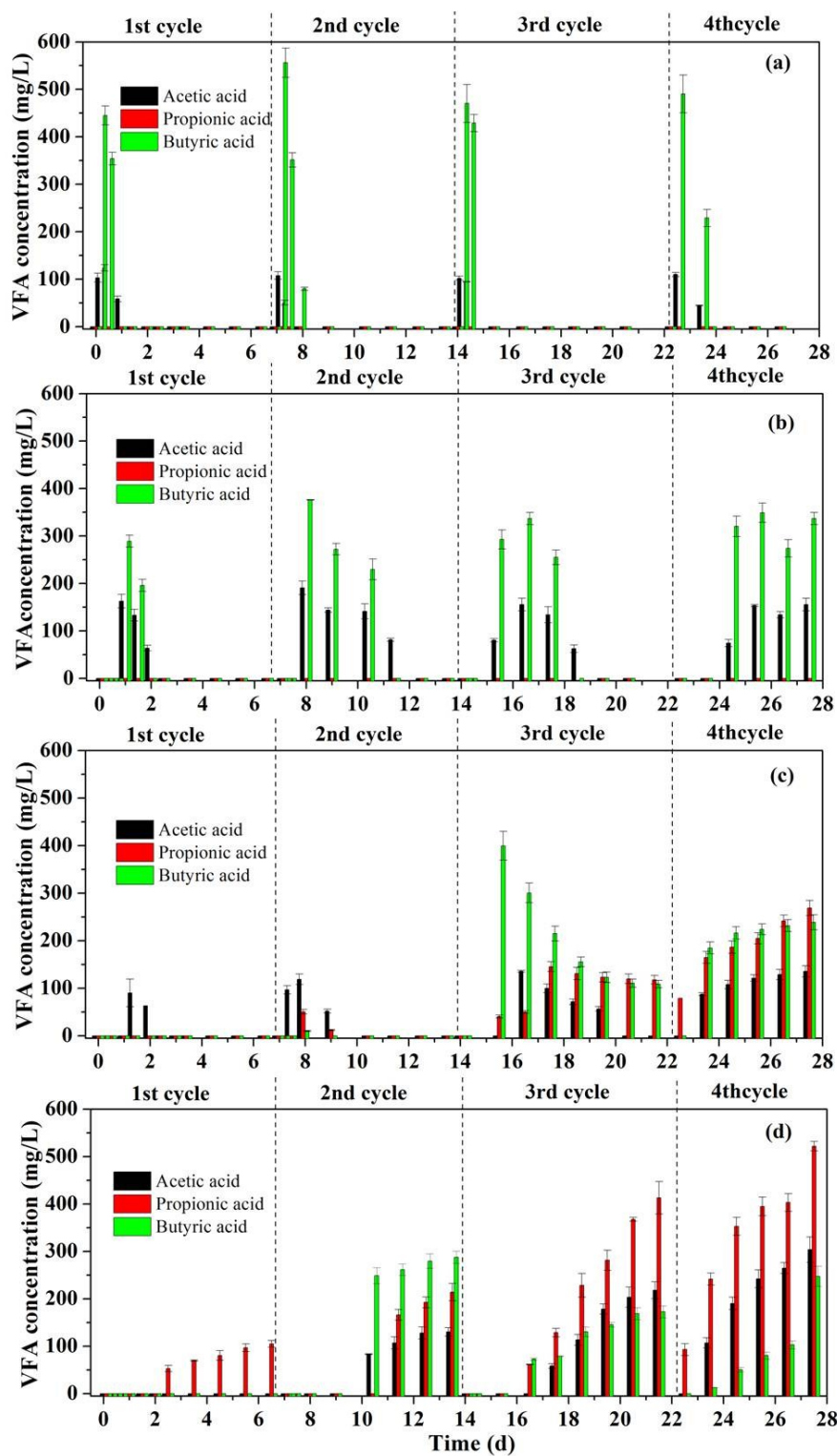


**Fig. S11** The main acidification products (including acetic, propionic and butyric acids) with time during four cycles after exposure to 0 (a), 10 (b), 30 (c), 120 (d) mg/L Ni<sup>2+</sup> ions. Error bars represent standard deviations of triplicate tests. 2 g/L glucose, pH 7.3, 115 rpm, 35 °C.

## References

1. H. Mu, X. Zheng, Y. G. Chen, H. Chen and K. Liu, Response of anaerobic granular sludge to a shock load of zinc oxide nanoparticles during biological wastewater treatment, *Environ. Sci. Technol.*, 2012, **46**, 5997-6003.
2. C. Sundberg, W. A. Al - Soud, M. Larsson, E. Alm, S. S. Yekta, B. H. Svensson, S. J. Sørensen and A. Karlsson, 454 pyrosequencing analyses of bacterial and archaeal richness in 21 full - scale biogas digesters, *FEMS Microbiol. Ecol.*, 2013, **85**, 612-626.
3. F. Guo and T. Zhang, Biases during DNA extraction of activated sludge samples revealed by high throughput sequencing, *Appl. Microbiol. Biotechnol.*, 2013, **97**, 4607-4616.
4. P. D. Schloss, S. L. Westcott, T. Ryabin, J. R. Hall, M. Hartmann, E. B. Hollister, R. A. Lesniewski, B. B. Oakley, D. H. Parks and C. J. Robinson, Introducing mothur: open-source, platform-independent, community-supported software for describing and comparing microbial communities, *Appl. Environ. Microbiol.*, 2009, **75**, 7537-7541.
5. F. Zhang, Y. Zhang, M. Chen and R. J. Zeng, Hydrogen supersaturation in thermophilic mixed culture fermentation, *Int. J. Hydrogen Energy*, 2012, **37**, 17809-17816.
6. H. Q. Li and J. Xu, A new correction method for determination on carbohydrates in lignocellulosic biomass, *Bioresour. Technol.*, 2013, **138**, 373-376.
7. , American Public Health Association, (18th ed). Washington, DC, Standard methods for the examination of water and wastewater, 2005.
8. H. L. Zhang, W. Fang, Y. P. Wang, G. P. Sheng, R. J. Zeng, W. W. Li and H. Q. Yu, Phosphorus removal in an enhanced biological phosphorus removal process: roles of extracellular polymeric substances, *Environ. Sci. Technol.*, 2013, **47**, 11482-11489.
9. Y. B. Zhang, X. L. An and X. Quan, Enhancement of sludge granulation in a zero valence iron packed anaerobic reactor with a hydraulic circulation, *Process Biochem.*, 2011, **46**, 471-476.
10. L. Zhu, H. Y. Qi, Y. Kong, Y. W. Yu and X. Y. Xu, Component analysis of extracellular polymeric substances (EPS) during aerobic sludge granulation using FTIR and 3D-EEM technologies, *Bioresour. Technol.*, 2012, **124**, 455-459.

11. L. Ren, K. S. Hui and K. N. Hui, Self-assembled free-standing three-dimensional nickel nanoparticle/graphene aerogel for direct ethanol fuel cells, *J. Mater. Chem. A*, 2013, **1**, 5689-5694.
12. M. Z. Hu, J. H. He, M. Q. Yang, X. C. Hu, C. X. Yan and Z. X. Cheng, Hydrothermal synthesis of nanostructured flower-like Ni(OH)<sub>2</sub> particles and their excellent sensing performance towards low concentration HCN gas, *RSC Adv.*, 2015, **5**, 26823-26831.
13. A. Larimi and S. Alavi, Ceria-Zirconia supported Ni catalysts for partial oxidation of methane to synthesis gas, *Fuel*, 2012, **102**, 366-371.
14. L. L. Wang, L. F. Wang, X. M. Ren, X. D. Ye, W. W. Li, S. J. Yuan, M. Sun, G. P. Sheng, H. Q. Yu and X. K. Wang, pH dependence of structure and surface properties of microbial EPS, *Environ. Sci. Technol.*, 2012, **46**, 737-744.
15. B. M. Lee and J. Hur, Adsorption Behavior of Extracellular Polymeric Substances on Graphene Materials Explored by Fluorescence Spectroscopy and Two-Dimensional Fourier Transform Infrared Correlation Spectroscopy, *Environ. Sci. Technol.*, 2016, **50**, 7364-7372.
16. X. F. Sun, S. G. Wang, X. M. Zhang, J. P. Chen, X. M. Li, B. Y. Gao and Y. Ma, Spectroscopic study of Zn<sup>2+</sup> and Co<sup>2+</sup> binding to extracellular polymeric substances (EPS) from aerobic granules, *J. Colloid Interf. Sci.*, 2009, **335**, 11-17.